A&A 545, A61 (2012)
DOI: 10.1051/0004-6361/201219852

Astronomy & Astrophysics

Li I spectra in the 4.65–8.33 micron range: high-*L* states and oscillator strengths

S. Civiš[1], M. Ferus[1], P. Kubelík[1], V. E. Chernov[1,2], and E. M. Zanozina[3,1]

[1] J. Heyrovský Institute of Physical Chemistry, Academy of Sciences of the Czech Republic, Dolejškova 3, 18223 Prague 8, Czech Republic
e-mail: civis@jh-inst.cas.cz
[2] Voronezh State University, 394693 Voronezh, Russia
e-mail: chernov@niif.vsu.ru
[3] State Research Center of Russian Federation Troitsk Institute of Innovation and Fusion Research, 142190 Troitsk, Moscow Region, Russia

Received 20 June 2012 / Accepted 30 July 2012

ABSTRACT

Context. Infrared (IR) astronomy capacities have rapidly developed in recent years thanks to several ground- and space-based facilities. To take advantage of these capabilities efficiently, a large amount of atomic data (such as line wavenumber, excited-level energy values, and oscillator strengths) are needed. These data are incomplete, in particular, for lithium whose abundances are important for several astrophysical problems.
Aims. No laboratory-measured spectra of Li I have been reported for wavelengths longward of 6.6 microns. We aim to find new Li I lines in the 4.65–8.33 microns range due to transitions between states with high orbital momentum ($l \geq 4$) and to determine the excitation energies of these states.
Methods. The Li I lines were studied using the time-resolved Fourier transform infrared spectroscopy of a plasma created by the laser ablation of a LiF target in a vacuum. The classification of the lines was performed by accounting for oscillator strengths (f-values) calculated using quantum defect theory (QDT). The adequacy of QDT for these calculations was checked by comparison with the available experimental and theoretical results.
Results. We report four new Li I lines in the 900–2200 cm^{-1} range that allow us to extract the excitation energies of the 6g, 6h, and 7h states of Li I, which have not been measured before. We also provide a large list of QDT-calculated f-values for Li I in the range of 1–20 microns.

Key words. atomic data – line: identification – methods: laboratory – techniques: spectroscopic – infrared: general

1. Introduction

The observation of lithium spectral lines in stellar atmospheres provide the astrophysicists with important information about primordial (Big Bang) nucleosynthesis, the evolution, mixing, and spallation processes in stars, stellar rotation history, and even the formation of planets (Lambert 1993; Carlsson et al. 1994; Iocco et al. 2009; Meléndez et al. 2010).

The identification of the main source of Li in the Galaxy (primordial nucleosynthesis, stars, or Galactic cosmic rays) remains unclear (Prantzos 2012). The phenomenon of "lithium depletion" (the so-called "cosmological lithium problem", see, e.g., Sbordone et al. 2010; Monaco et al. 2010) observed in Sun-like stars, consists in a disagreement between the primordial lithium abundance predicted from standard Big Bang nucleosynthesis and its abundance corresponding to the Spite plateau (Spite & Spite 1982a,b).

It is assumed that the lithium depletion is connected with mixing the different temperature layers by diffusion, meridional circulation, and internal gravity waves (Pace et al. 2012). Some models claim a rotational mixing mechanism and predict stronger Li depletion for planet-hosting stars (Bouvier 2008; Israelian et al. 2009; Eggenberger et al. 2012). Thus, the Li abundance is an effective indicator of mixing processes in stars and therefore spectroscopic observations of Li in metal-poor stars (including relatively old solar-type stars) are needed (Canto Martins et al. 2011; Pace et al. 2012; Nissen & Schuster 2012).

For cool low-mass objects, the spectroscopic detection of lithium can be applied to determine their mass or age (Yee & Jensen 2010). Recent high-resolution spectroscopic studies have shown lithium enhancements in the atmospheres of some young cool stars that have been classified as lithium-rich K- and M-type giants (Alcalá et al. 2011) and some dwarfs (Koch et al. 2011; Monaco et al. 2012).

Cool objects such as dwarfs, disks, or planets and the extended atmospheres of evolved stars are extensively being studied by infrared (IR) astronomy (Lyubchik et al. 2004, 2007; Kerber et al. 2009). Though the current space-born IR spectrographs (e.g., *Herschel*, *Spitzer*, AKARI) have a spectral resolution $R \sim 100$–1000), the forthcoming spatial and airborne (SOFIA, SPICA) telescopes are expected to have a much higher resolution. The great advantages of Fourier transform infrared (FTIR) spectroscopy, such as its constant high resolution and energy throughput, have made the IR spectral region more accessible for laboratory spectral measurements (Nilsson 2009). However, the powerful capacities of IR astronomy cannot be fully utilized without detailed spectroscopic information on

Table 1. Observed new lines of Li I and their identifications.

ν	*FWHM*	*I*	*SNR*	Lower level		Upper level		$\log(\bar{g}\bar{f})$
(cm^{-1})	(cm^{-1})	(arb. u.)		*nl*	Energy, (cm^{-1})	*nl*	Energy, (cm^{-1})	(multiplet value)
1341.211(5)	0.068(19)	6.19×10^3	7.39	5g	39097.941(6) [1]	6h	40 439.152(21) 40 438.12 [2]	3.41
1341.494(8)	0.076(24)	3.84×10^3	3.55	5f	39097.503(15) [1]	6g	40 438.997(40) 40 437.91 [2]	2.81
1457.735(7)	0.063(21)	3.59×10^3	6.66	4s	35012.0326(10) [1]	4p	36 469.7943(15) [1]	1.18
2149.871(11)	0.051(51)	6.01×10^1	3.56	5g	39097.941(6) [1]	7h	41 247.812(26) 41 246.98 [2]	1.29

References. [1] Radziemski et al. (1995); [2] Chen & Wang (2005).

atomic line features (in particular, wavelengths and oscillator strengths) in the IR region (Biémont 1994; Johansson 2005; Pickering et al. 2011; see the references in Civiš et al. 2012a, for more references on IR space- and ground-based astronomy).

The majority of Li abundance studies are based on the analysis of the resonance Li I 670.8 nm line only, while some other lines, e.g., the 610.4 nm line (Merchant 1967; Bonifacio & Molaro 1998) or the 812.6 nm line (Yakovina et al. 2003) can be potentially good lithium-abundance indicators. The most comprehensive, to the authors' knowledge, Li I line list to date was presented by Radziemski et al. (1995); it covers the 1800–31 000 cm^{-1} (5.6–3.2 micron) range. No lines with wavelengths longer than 5.6 micron have been reported in the literature.

The most prominent lines in atomic metal spectra below 1800 cm^{-1} are typically due to the radiative transitions between the atomic states with high orbital momentum $l \geq 4$. However, except for the 5g term measured by Litzen (1970), the high-l levels, i.e. the ng (with $n > 5$) or nh states, have never been observed for Li I.

The present work aims to fill this gap in the available Li I level and line lists. We measure the emission spectra of Li I in the 1300–2200 cm^{-1} range and, from these spectra, extract the energies of the 6g, 6h and 7h levels. We also present the oscillator strengths of the dipole transitions between the observed levels. These f-values are calculated using the quantum defect theory (QDT) technique. This work is a continuation of our previous studies (Civiš et al. 2012a,b).

2. Methods

We study the IR emission spectrum of Li I, which was measured using high-resolution FTIR spectroscopy of the plasma formed by the laser ablation of an LiF target. The sample surface was irradiated by a high-repetition-rate, pulsed, nanosecond ArF laser (λ = 193 nm, laser pulse width 12 ns, frequency 1.0 kHz, output energy 15 mJ) in a vacuum (10^{-2} Torr). The emission from the plasma was focused into the spectrometer by a ZnSe (127 mm) lens for the 900–1600 cm^{-1} spectral range and by a CaF_2 (100 mm) lens for the 1600–2200 cm^{-1} range. Two different detectors (MCT and InSb) and two beamsplitters (KBr and CaF_2) were used to cover the measured spectral range. The atomic spectra were measured by a Bruker 120 FTIR spectrometer, which was specially modified for time-resolved measurements and calibrated against the internally stabilized HeNe laser. More details on the experimental setup are given in our previous papers (Kawaguchi et al. 2008; Civiš et al. 2010a; Civiš et al. 2010b, 2011c).

Because the g ($n > 5$) and h levels are absent from the available line lists, we started from the approximate energies of the n'g- and n'' h-states obtained from the Rydberg formula to identify the lines involving these levels. We then refined these level energies using the measured line wavenumbers. In the cases of transitions with close wavenumbers, we compared the oscillator strengths of the lines, which were calculated using single-channel quantum defect theory (QDT). This theory has already been shown to be efficient in calculating the first- (Alcheev et al. 2002) and second-order (Chernov et al. 2005; Akindinova et al. 2009) matrix elements in atoms and molecules. To show that QDT calculations of dipole transition matrix elements are sufficient for our line identification, we compare some QDT-calculated Rb oscillator strengths with experimental and theoretical data available in the literature.

Tables 2 and 3 compare our QDT-calculated f-values with values taken from different sources. In Table 2, we compare our f-values ($f \times 100$) with oscillator strengths obtained from some available experimental or calculated lifetimes. The f-values were extracted from the reported lifetimes in a way similar to that used in our previous work (Civiš et al. 2010b). Table 3 compares our result with the Li I f-values available from NIST ASD (National Institute of Standards and Technology Atomic Spectra Database; Ralchenko et al. 2011), which lists the data from the reviewing paper (Wiese & Fuhr 2009). As in our previous works (Civiš et al. 2010a; Civiš et al. 2010b, 2011b; Civiš et al. 2012a,b), the overall agreement of our QDT calculations with the results available in other sources is quite satisfactory and this agreement show the QDT calculations to be adequate for the identification of the observed transitions.

3. Results and discussion

In their quite comprehensive study of the Li I spectrum, Radziemski et al. (1995) reported 34 lines in the 1829–30 925 cm^{-1} range. We observed only one line (2149.871 cm^{-1}) not reported by Radziemski et al. (1995). In total, in the range 900–2200 cm^{-1}, we found four lines that had not been previously measured. These are listed in Table 1 together with the other observed lines and their parameters (wavenumbers, full widths at half-maxima, measured intensities, and signal-to-noise ratios) and identification in Table 1. A part of the recorded spectra is shown in Fig. 1, where two $5l'$–$6l''$ transition lines are shown ($l' = 4$, $l'' = 5$).

On the basis of the known value of the 5g level, we extract three new levels of Li I, which are presented in Table 1 in the upper level column (without references), together with other measured or calculated values (with references). The 6g, 6h, and 7h

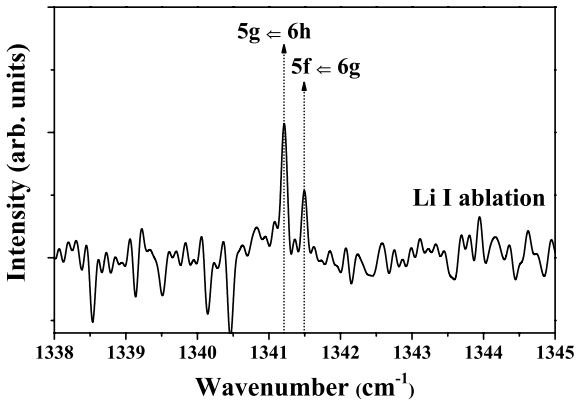

Fig. 1. A part of Li I emission spectrum with the transitions between the states with $n = 5$ and 6.

levels have never been measured before. We can compare them only with the variational calculations of Chen & Wang (2005). We note that for the 5g level the energy value 39 096.75 cm^{-1} calculated by Chen & Wang (2005) differs approximately by 1 cm^{-1} from the measured values of 39 097.941(6) (Radziemski et al. 1995) and 39 097.96 (Litzen 1970). As can be seen from Table 1, our values are also shifted approximately by 1 cm^{-1} compared to the results of Chen & Wang (2005). Given the above considerations, we consider our values from Table 1 as recommended ones.

Unfortunately, our resolution is not enough to resolve the fine structure of the observed Li I lines. According to (Radziemski et al. 1995), the 4p level has a fine splitting about 0.04 cm^{-1}, while the fine splitting of the high-l levels should be much more lower. Thus, the j values are not specified in Table 1 and the presented $\log(\bar{g}\bar{f})$ values are those averaged over the multiplets.

Given the above-mentioned agreement of our QDT calculation with the dipole transition matrix elements, we present in Table 4 the matrix elements (f- and A-values) for the transition involving the nd, nf, ng, and nh states of Li I. In particular, this A-value list was used to identify the observed lines according to their relative intensities.

4. Conclusion

This work continues a series of FTIR spectroscopy studies of IR spectra of metal atoms (Civiš et al. 2010a; Civiš et al. 2010b, 2011c,a; Civiš et al. 2012a,b). We have reported the results of laboratory measurements for four new Li I lines in the 900–2200 cm^{-1} range. To our knowledge, there are no laboratory-measured Li I spectra below 1800 cm^{-1} (above 5.6 microns). The classification of the lines was performed by accounting for oscillator strengths (f-values) calculated using quantum defect theory (QDT). The comparison of the QDT calculations with the available experimental and theoretical results proves that QDT is an adequate tool for calculating dipole transition matrix elements. The recorded spectra have allowed us to extract the excitation energies of the 6g, 6h, and 7h states of Li I, which had not been measured before.

Acknowledgements. This work was financially supported by the Grant Agency of the Academy of Sciences of the Czech Republic (grant No. IAAX00100903), by the Ministry of Finance of the Czech Republic (Project ECPF:049/4V) and the Ministry of Education, Youth, and Sports of the Czech Republic (grant No. LM2010014).

Table 2. Comparison of Li I oscillator strengths ($f \times 100$) with strengths obtained from previously published experimental or calculated lifetimes.

		Other sources	
Transition	Present work	Experiment	Theory
$2s_{\frac{1}{2}}$–$2p_{\frac{3}{2}}$	49.5	49.82 ± 0.11 [1]	49.58 [3]
		50.2 ± 1.5 [2]	49.797 [4]
		50.04 ± 0.30 [5]	49.82 [6]
$2s_{\frac{1}{2}}$–$2p_{\frac{1}{2}}$	24.7	24.91 ± 0.06 [1]	24.80 [3]
		25.1 ± 0.7 [2]	24.899 [4]
		25.02 ± 0.15 [5]	24.91 [6]
$2p_{\frac{3}{2}}$–$3s_{\frac{1}{2}}$	11.1		11.00 [3]
$2p_{\frac{1}{2}}$–$3s_{\frac{1}{2}}$	11.1		11.00 [3]
$2s_{\frac{1}{2}}$–$3p_{\frac{1}{2}}$	0.151	0.159 ± 0.006 [7]	0.152 [3]
$2s_{\frac{1}{2}}$–$3p_{\frac{3}{2}}$	0.302	0.317 ± 0.013 [7]	0.304 [3]
$3s_{\frac{1}{2}}$–$3p_{\frac{1}{2}}$	40.4	42.4 ± 1.7 [7]	40.60 [3]
$3s_{\frac{1}{2}}$–$3p_{\frac{3}{2}}$	80.9	84.9 ± 3.3 [7]	81.21 [3]
$2p_{\frac{1}{2}}$–$3d_{\frac{3}{2}}$	64.4	62.5 ± 2.1 [2]	63.65 [3]
$2p_{\frac{3}{2}}$–$3d_{\frac{3}{2}}$	6.44	6.3 ± 0.2 [2]	6.36 [3]
$2p_{\frac{3}{2}}$–$3d_{\frac{5}{2}}$	57.9	56.3 ± 1.9 [2]	57.95 [3]
$3p_{\frac{3}{2}}$–$3d_{\frac{5}{2}}$	6.70	6.5 ± 0.2 [2]	6.70 [3]
$3p_{\frac{1}{2}}$–$3d_{\frac{3}{2}}$	7.44	7.2 ± 0.2 [2]	7.36 [3]
$3p_{\frac{3}{2}}$–$3d_{\frac{3}{2}}$	0.744	0.72 ± 0.02 [2]	0.736 [3]
$2p_{\frac{3}{2}}$–$4s_{\frac{1}{2}}$	1.29	1.37 ± 0.04 [2]	1.28 [3]
		1.29 ± 0.04 [8]	
$2p_{\frac{1}{2}}$–$4s_{\frac{1}{2}}$	1.29	1.37 ± 0.04 [2]	1.28 [3]
		1.29 ± 0.04 [8]	
$3p_{\frac{3}{2}}$–$4s_{\frac{1}{2}}$	22.3	23.72 ± 0.72 [2]	22.21 [3]
		22.3 ± 0.7 [8]	
$3p_{\frac{1}{2}}$–$4s_{\frac{1}{2}}$	22.3	23.72 ± 0.72 [2]	22.21 [3]
		22.3 ± 0.7 [8]	
$2p_{\frac{3}{2}}$–$5s_{\frac{1}{2}}$	0.433	0.430 ± 0.017 [2]	0.431 [3]
		0.44 ± 0.04 [8]	
$2p_{\frac{1}{2}}$–$5s_{\frac{1}{2}}$	0.433	0.430 ± 0.017 [2]	0.431 [3]
		0.44 ± 0.04 [8]	
$3p_{\frac{3}{2}}$–$5s_{\frac{1}{2}}$	2.59	2.58 ± 0.10 [2]	2.582 [3]
		2.7 ± 0.2 [8]	
$3p_{\frac{1}{2}}$–$5s_{\frac{1}{2}}$	2.59	2.58 ± 0.10 [2]	2.582 [3]
		2.7 ± 0.2 [8]	
$4p_{\frac{3}{2}}$–$5s_{\frac{1}{2}}$	33.6	33.4 ± 1.3 [2]	33.42 [3]
		34. ± 3. [8]	
$4p_{\frac{1}{2}}$–$5s_{\frac{1}{2}}$	33.6	33.4 ± 1.3 [2]	33.42 [3]
		34. ± 3. [8]	

References. [1] Beam-gas-laser spectroscopy (Volz et al. 1996); [2] measurements by using pulsed dye laser excitation and a single-photon-counting technique (Hansen 1983); [3] realistic calculations including the core polarization, spin-orbit interaction, and blackbody radiation (Theodosiou 1984); [4] high precision calculations using variational wave functions in Hylleraas coordinates (Yan & Drake 1995); [5] photoassociative spectroscopy of ultracold lithium (McAlexander et al. 1995); [6] realistic all-oder calculations (Blundell et al. 1989); [7] the method of level-crossing spectroscopy (Nagourney et al. 1978); [8] measurements with metal-vapor spectroscopic oven based on the heat-pipe principle (Boyd et al. 1980).

References

Akindinova, E. V., Chernov, V. E., Kretinin, I. Y., & Zon, B. A. 2009, Phys. Rev. A, 79, 032506

Alcalá, J. M., Biazzo, K., Covino, E., Frasca, A., & Bedin, L. R. 2011, A&A, 531, L12
Alcheev, P. G., Chernov, V. E., & Zon, B. A. 2002, J. Mol. Spectrosc., 211, 71
Biémont, E. 1994, in Infrared Solar Physics, eds. D. M. Rabin, J. T. Jefferies, & C. Lindsey (Dordrecht, The Netherlands: Kluwer Academic Publ.), IAU Symp., 154, 501
Blundell, S., Johnson, W., Liu, Z., & Sapirstein, J. 1989, Phys. Rev. A, 40, 2233
Bonifacio, P., & Molaro, P. 1998, ApJ, 500, L175
Bouvier, J. 2008, A&A, 489, L53
Boyd, R. W., Dodd, J. G., Krasinski, J., & Stroud, C. R. 1980, Opt. Lett., 5, 117
Canto Martins, B. L., Lèbre, A., Palacios, A., et al. 2011, A&A, 527, A94
Carlsson, M., Rutten, R. J., Bruls, J. H. M. J., & Shchukina, N. G. 1994, A&A, 288, 860
Chen, C., & Wang, Z.-W. 2005, Commun. Theor. Phys., 43, 886
Chernov, V. E., Dorofeev, D. L., Kretinin, I. Y., & Zon, B. A. 2005, Phys. Rev. A, 71, 022505
Civiš, S., Matulková, I., Cihelka, J., et al. 2010a, Phys. Rev. A, 81, 012510
Civiš, S., Matulková, I., Cihelka, J., et al. 2010b, Phys. Rev. A, 82, 022502
Civiš, S., Kubelík, P., Jelínek, P., Chernov, V. E., & Knyazev, M. Y. 2011a, J. Phys. B, 44, 225006
Civiš, S., Matulková, I., Cihelka, J., et al. 2011b, J. Phys. B, 44, 105002
Civiš, S., Matulková, I., Cihelka, J., et al. 2011c, J. Phys. B, 44, 025002
Civiš, S., Ferus, M., Kubelík, P., Jelinek, P., & Chernov, V. E. 2012a, A&A, 541, A125
Civiš, S., Ferus, M., Kubelík, P., et al. 2012b, A&A, 542, A35
Eggenberger, P., Haemmerle, L., Meynet, G., & Maeder, A. 2012, A&A, 539, A70
Filippov, A. 1931, Z. Phys. A, 69, 526
Fischer, C., Saparov, M., Gaigalas, G., & Godefroid, M. 1998, ADNDT, 70, 119
Hansen, W. 1983, J. Phys. B, 16, 933
Iocco, F., Mangano, G., Miele, G., Pisanti, O., & Serpico, P. D. 2009, Phys. Rep., 472, 1
Israelian, G., Mena, E. D., Santos, N. C., et al. 2009, Nature, 462, 189
Johansson, S. 2005, in High Resolution Infrared Spectroscopy In Astronomy, Proceedings, eds. H. U. Kaufl, R. Siebenmorgen, & A. Moorwood (Heidelberger, Berlin: Springer-Verlag), ESO Astrophysics Symp., 62
Kawaguchi, K., Sanechika, N., Nishimura, Y., et al. 2008, Chem. Phys. Lett., 463, 38
Kerber, F., Nave, G., Sansonetti, C. J., & Bristow, P. 2009, Phys. Scr., T134, 014007
Koch, A., Lind, K., & Rich, R. M. 2011, ApJ, 738, 29
Lambert, D. L. 1993, Phys. Scr. T, 47, 186
Litzen, U. 1970, Phys. Scr., 1, 253
Lyubchik, Y., Jones, H. R. A., Pavlenko, Y. V., et al. 2004, A&A, 416, 655
Lyubchik, Y., Jones, H. R. A., Pavlenko, Y. V., et al. 2007, A&A, 473, 257
McAlexander, W. I., Abraham, E. R. I., Ritchie, N. W. M., et al. 1995, Phys. Rev. A, 51, R871
Meléndez, J., Ramírez, I., Casagrande, L., et al. 2010, Astrophys. Space. Sci., 328, 193
Merchant, A. E. 1967, ApJ, 147, 587
Monaco, L., Bonifacio, P., Sbordone, L., Villanova, S., & Pancino, E. 2010, A&A, 519, L3
Monaco, L., Villanova, S., Bonifacio, P., et al. 2012, A&A, 539, A157
Nagourney, W., Happer, W., & Lurio, A. 1978, Phys. Rev. A, 17, 1394
Nilsson, H. 2009, Phys. Scr. T, 134, 014009
Nissen, P. E., & Schuster, W. J. 2012, A&A, 543, A28
Pace, G., Castro, M., Meléndez, J., Théado, S., & do Nascimento Jr., J.-D. 2012, A&A, 541, A150
Peach, G., Saraph, H., & Seaton, M. 1988, J. Phys. B, 21, 3669
Pestka, G., & Woznicki, W. 1996, Chem. Phys. Lett., 255, 281
Pickering, J., Blackwell-Whitehead, R., Thorne, A., Ruffoni, M., & Holmes, C. 2011, Can. J. Phys., 89, 387
Prantzos, N. 2012, A&A, 542, A67
Qu, L. H., Wang, Z. W., & Guan, X. X. 1997, Chin. Phys. Lett., 14, 732
Qu, L. H., Wang, Z. W., & Li, B. W. 1999, Opt. Commun., 162, 223
Radziemski, L. J., Engleman, R., & Brault, J. W. 1995, Phys. Rev. A, 52, 4462
Ralchenko, Y., Kramida, A., Reader, J., & NIST ASD Team 2011, NIST Atomic Spectra Database, version 4.1.0
Sbordone, L., Bonifacio, P., Caffau, E., et al. 2010, A&A, 522, A26
Spite, F., & Spite, M. 1982a, A&A, 115, 357
Spite, M., & Spite, F. 1982b, Nature, 297, 483
Theodosiou, C. E. 1984, Phys. Rev. A, 30, 2881
Volz, U., Majerus, M., Liebel, H., Schmitt, A., & Schmoranzer, H. 1996, Phys. Rev. Lett., 76, 2862
Wiese, W. L., & Fuhr, J. R. 2009, J. Phys. Chem. Ref. Data, 38, 565
Yakovina, L., Pavlenko, Y., & Abia, C. 2003, Astrophys. Space Sci., 288, 279
Yan, Z.-C., & Drake, G. W. F. 1995, Phys. Rev. A, 52, R4316
Yee, J. C., & Jensen, E. L. N. 2010, ApJ, 711, 303

Table 3. Comparison of oscillator strengths (f-values) for several transitions in Li I with known values from the compilation by Wiese & Fuhr (2009).

Transition	This work	Other works	
$2s_{\frac{1}{2}}$–$2p_{\frac{3}{2}}$	4.95E-1	4.9798E-1	[1] LS
$2s_{\frac{1}{2}}$–$2p_{\frac{1}{2}}$	2.47E-1	2.4898E-1	[1] LS
$2s_{\frac{1}{2}}$–$3p_{\frac{3}{2}}$	3.04E-3	3.141E-3	[2] LS
$2s_{\frac{1}{2}}$–$3p_{\frac{1}{2}}$	1.52E-3	1.570E-3	[2] LS
$2s_{\frac{1}{2}}$–$4p_{\frac{3}{2}}$	2.75E-3	2.812E-3	[3] LS
$2s_{\frac{1}{2}}$–$4p_{\frac{1}{2}}$	1.38E-3	1.406E-3	[3] LS
$2s_{\frac{1}{2}}$–$5p_{\frac{3}{2}}$	1.65E-3	1.733E-3	[6]
$2s_{\frac{1}{2}}$–$5p_{\frac{1}{2}}$	8.26E-4	8.863E-4	[6]
$2s_{\frac{1}{2}}$–$6p_{\frac{3}{2}}$	1.01E-3	1.054E-3	[6]
$2s_{\frac{1}{2}}$–$6p_{\frac{1}{2}}$	5.07E-4	5.269E-4	[6]
$2s_{\frac{1}{2}}$–$7p_{\frac{3}{2}}$	6.62E-4	6.749E-4	[6]
$2s_{\frac{1}{2}}$–$7p_{\frac{1}{2}}$	3.31E-4	3.373E-4	[6]
$2s_{\frac{1}{2}}$–$8p_{\frac{3}{2}}$	4.61E-4	4.582E-4	[6]
$2s_{\frac{1}{2}}$–$8p_{\frac{1}{2}}$	2.31E-4	2.291E-4	[6]
$2s_{\frac{1}{2}}$–$9p_{\frac{3}{2}}$	3.17E-4	3.241E-4	[6]
$2s_{\frac{1}{2}}$–$9p_{\frac{1}{2}}$	1.58E-4	1.620E-4	[6]
$2s_{\frac{1}{2}}$–$10p_{\frac{1}{2}}$	1.19E-4	1.74E-4	[5]
$2s_{\frac{1}{2}}$–$10p_{\frac{3}{2}}$	2.38E-4	3.49E-4	[5]
$2s_{\frac{1}{2}}$–$11p_{\frac{3}{2}}$	2.41e-4	2.73E-4	[5]
$2s_{\frac{1}{2}}$–$11p_{\frac{1}{2}}$	1.20e-4	1.37E-4	[5]
$2s_{\frac{1}{2}}$–$12p_{\frac{1}{2}}$	0.68e-4	1.10E-4	[5]
$2s_{\frac{1}{2}}$–$12p_{\frac{3}{2}}$	1.35e-4	2.20E-4	[5]
$2s_{\frac{1}{2}}$–$13p_{\frac{1}{2}}$	5.53e-5	8.91E-5	[5]
$2s_{\frac{1}{2}}$–$13p_{\frac{3}{2}}$	1.11e-4	1.78E-4	[5]
$2p_{\frac{3}{2}}$–$3s_{\frac{1}{2}}$	1.11E-1	1.1050E-1	[2] LS
$2p_{\frac{1}{2}}$–$3s_{\frac{1}{2}}$	1.11E-1	1.1051E-1	[2] LS
$2p_{\frac{3}{2}}$–$3d_{\frac{5}{2}}$	5.79E-1	5.747E-1	[1] LS
$2p_{\frac{1}{2}}$–$3d_{\frac{3}{2}}$	6.44E-1	6.3858E-1	[1] LS
$2p_{\frac{3}{2}}$–$3d_{\frac{3}{2}}$	6.44E-2	6.3857E-2	[1] LS
$2p_{\frac{3}{2}}$–$4s_{\frac{1}{2}}$	1.29E-2	1.283E-2	[2] LS
$2p_{\frac{1}{2}}$–$4s_{\frac{1}{2}}$	1.29E-2	1.283E-2	[2] LS
$2p_{\frac{3}{2}}$–$4d_{\frac{5}{2}}$	1.11E-1	1.107E-1	[3] LS
$2p_{\frac{1}{2}}$–$4d_{\frac{3}{2}}$	1.24E-1	1.230E-1	[3] LS
$2p_{\frac{3}{2}}$–$4d_{\frac{3}{2}}$	1.24E-2	1.230E-2	[3] LS
$2p_{\frac{3}{2}}$–$5s_{\frac{1}{2}}$	4.33E-3	4.34E-3	[4] LS
$2p_{\frac{1}{2}}$–$5s_{\frac{1}{2}}$	4.33E-3	4.34E-3	[4] LS
$2p_{\frac{3}{2}}$–$5d_{\frac{5}{2}}$	4.20E-2	4.16E-2	[4] LS
$2p_{\frac{1}{2}}$–$5d_{\frac{3}{2}}$	4.66E-2	4.63E-2	[4] LS
$2p_{\frac{3}{2}}$–$5d_{\frac{3}{2}}$	4.66E-3	4.63E-3	[4] LS
$2p_{\frac{3}{2}}$–$6s_{\frac{1}{2}}$	2.04E-3	2.05E-3	[4] LS
$2p_{\frac{1}{2}}$–$6s_{\frac{1}{2}}$	2.04E-3	2.05E-3	[4] LS
$2p_{\frac{3}{2}}$–$6d_{\frac{5}{2}}$	2.08E-2	2.055E-2	[6] LS
$2p_{\frac{1}{2}}$–$6d_{\frac{3}{2}}$	2.31E-2	2.283E-2	[6] LS
$2p_{\frac{3}{2}}$–$6d_{\frac{3}{2}}$	2.31E-3	2.283E-3	[6] LS
$2p_{\frac{3}{2}}$–$7s_{\frac{1}{2}}$	1.14E-3	1.15E-3	[4] LS
$2p_{\frac{1}{2}}$–$7s_{\frac{1}{2}}$	1.14E-3	1.15E-3	[4] LS
$2p_{\frac{3}{2}}$–$7d_{\frac{5}{2}}$	1.20E-2	1.183E-2	[6] LS
$2p_{\frac{1}{2}}$–$7d_{\frac{3}{2}}$	1.33E-2	1.314E-2	[6] LS
$2p_{\frac{3}{2}}$–$7d_{\frac{3}{2}}$	1.33E-3	1.314E-3	[6] LS

Table 3. continued.

Transition	This work	Other works	
$2p_{\frac{3}{2}}$–$8s_{\frac{1}{2}}$	7.07E-4	7.11E-4	[4] LS
$2p_{\frac{1}{2}}$–$8s_{\frac{1}{2}}$	7.07E-4	7.11E-4	[4] LS
$2p_{\frac{3}{2}}$–$8d_{\frac{5}{2}}$	7.55E-3	7.519E-3	[6] LS
$2p_{\frac{1}{2}}$–$8d_{\frac{3}{2}}$	8.39E-3	8.354E-3	[6] LS
$2p_{\frac{3}{2}}$–$8d_{\frac{3}{2}}$	8.39E-4	8.354E-4	[6] LS
$2p_{\frac{3}{2}}$–$9d_{\frac{5}{2}}$	5.09E-3	5.090E-3	[6] LS
$2p_{\frac{1}{2}}$–$9d_{\frac{3}{2}}$	5.66E-3	5.656E-3	[6] LS
$2p_{\frac{3}{2}}$–$9d_{\frac{3}{2}}$	5.66E-4	5.656E-4	[6] LS
$3s_{\frac{1}{2}}$–$3p_{\frac{3}{2}}$	8.09E-1	8.102E-1	[2] LS
$3s_{\frac{1}{2}}$–$3p_{\frac{1}{2}}$	4.04E-1	4.051E-1	[2] LS
$3s_{\frac{1}{2}}$–$4p_{\frac{3}{2}}$	2.74E-5	2.4E-5	[3], [4] LS
$3s_{\frac{1}{2}}$–$4p_{\frac{1}{2}}$	1.38E-5	1.2E-5	[3], [4] LS
$3s_{\frac{1}{2}}$–$5p_{\frac{3}{2}}$	8.49E-4	8.68E-4	[4] LS
$3s_{\frac{1}{2}}$–$5p_{\frac{1}{2}}$	4.25E-4	4.34E-4	[4] LS
$3s_{\frac{1}{2}}$–$6p_{\frac{3}{2}}$	7.43E-4	7.54E-4	[4] LS
$3s_{\frac{1}{2}}$–$6p_{\frac{1}{2}}$	3.72E-4	3.77E-4	[4] LS
$3s_{\frac{1}{2}}$–$7p_{\frac{3}{2}}$	5.48E-4	5.51E-4	[4] LS
$3s_{\frac{1}{2}}$–$7p_{\frac{1}{2}}$	2.74E-4	2.75E-4	[4] LS
$3s_{\frac{1}{2}}$–$8p_{\frac{3}{2}}$	4.10E-4	3.95E-4	[4] LS
$3s_{\frac{1}{2}}$–$8p_{\frac{1}{2}}$	2.05E-4	1.97E-4	[4] LS
$3p_{\frac{3}{2}}$–$3d_{\frac{5}{2}}$	6.70E-2	6.62E-2	[2] LS
$3p_{\frac{1}{2}}$–$3d_{\frac{3}{2}}$	7.45E-2	7.36E-2	[2] LS
$3p_{\frac{3}{2}}$–$3d_{\frac{3}{2}}$	7.45E-3	7.36E-3	[2] LS
$3p_{\frac{3}{2}}$–$4s_{\frac{1}{2}}$	2.23E-1	2.230E-1	[2] LS
$3p_{\frac{1}{2}}$–$4s_{\frac{1}{2}}$	2.23E-1	2.230E-1	[2] LS
$3p_{\frac{3}{2}}$–$4d_{\frac{5}{2}}$	4.71E-1	4.704E-1	[3] LS
$3p_{\frac{1}{2}}$–$4d_{\frac{3}{2}}$	5.23E-1	5.227E-1	[3] LS
$3p_{\frac{3}{2}}$–$4d_{\frac{3}{2}}$	5.23E-2	5.227E-2	[3] LS
$3p_{\frac{3}{2}}$–$5s_{\frac{1}{2}}$	2.59E-2	2.60E-2	[4] LS
$3p_{\frac{1}{2}}$–$5s_{\frac{1}{2}}$	2.59E-2	2.60E-2	[4] LS
$3p_{\frac{3}{2}}$–$5d_{\frac{5}{2}}$	1.17E-1	1.17E-1	[4] LS
$3p_{\frac{1}{2}}$–$5d_{\frac{3}{2}}$	1.30E-1	1.30E-1	[4] LS
$3p_{\frac{3}{2}}$–$5d_{\frac{3}{2}}$	1.30E-2	1.30E-2	[4] LS
$3p_{\frac{3}{2}}$–$6s_{\frac{1}{2}}$	8.87E-3	8.88E-3	[4] LS
$3p_{\frac{1}{2}}$–$6s_{\frac{1}{2}}$	8.87E-3	8.88E-3	[4] LS
$3p_{\frac{3}{2}}$–$6d_{\frac{5}{2}}$	4.90E-2	4.90E-2	[4] LS
$3p_{\frac{1}{2}}$–$6d_{\frac{3}{2}}$	5.45E-2	5.44E-2	[4] LS
$3p_{\frac{3}{2}}$–$6d_{\frac{3}{2}}$	5.45E-3	5.44E-3	[4] LS
$3p_{\frac{3}{2}}$–$7s_{\frac{1}{2}}$	4.26E-3	4.27E-3	[4] LS
$3p_{\frac{1}{2}}$–$7s_{\frac{1}{2}}$	4.26E-3	4.27E-3	[4] LS
$3p_{\frac{3}{2}}$–$7d_{\frac{5}{2}}$	2.58E-2	2.58E-2	[4] LS
$3p_{\frac{1}{2}}$–$7d_{\frac{3}{2}}$	2.87E-2	2.87E-2	[4] LS
$3p_{\frac{3}{2}}$–$7d_{\frac{3}{2}}$	2.87E-3	2.87E-3	[4] LS
$3p_{\frac{3}{2}}$–$8s_{\frac{1}{2}}$	2.43E-3	2.44E-3	[4] LS
$3p_{\frac{1}{2}}$–$8s_{\frac{1}{2}}$	2.43E-3	2.44E-3	[4] LS
$3p_{\frac{3}{2}}$–$8d_{\frac{5}{2}}$	1.55E-2	1.55E-2	[4] LS
$3p_{\frac{1}{2}}$–$8d_{\frac{3}{2}}$	1.72E-2	1.72E-2	[4] LS
$3p_{\frac{3}{2}}$–$8d_{\frac{3}{2}}$	1.72E-3	1.72E-3	[4] LS
$3d_{\frac{5}{2}}$–$4p_{\frac{3}{2}}$	1.82E-2	1.797E-2	[3] LS
$3d_{\frac{3}{2}}$–$4p_{\frac{1}{2}}$	1.51E-2	1.498E-2	[3] LS
$3d_{\frac{3}{2}}$–$4p_{\frac{3}{2}}$	3.03E-3	2.996E-3	[3] LS

Table 3. continued.

Transition	This work	Other works	
$3d_{\frac{5}{2}}$–$4f_{\frac{7}{2}}$	9.68E-1	9.669E-1	[7] LS
$3d_{\frac{3}{2}}$–$4f_{\frac{5}{2}}$	1.02	1.015	[7] LS
$3d_{\frac{5}{2}}$–$4f_{\frac{5}{2}}$	4.84E-2	4.835E-2	[7] LS
$3d_{\frac{5}{2}}$–$5p_{\frac{3}{2}}$	3.48E-3	3.43E-3	[4] LS
$3d_{\frac{3}{2}}$–$5p_{\frac{1}{2}}$	2.90E-3	2.86E-3	[4] LS
$3d_{\frac{3}{2}}$–$5p_{\frac{3}{2}}$	5.81E-4	5.72E-4	[4] LS
$3d_{\frac{5}{2}}$–$5f_{\frac{7}{2}}$	1.50E-1	1.496E-1	[7] LS
$3d_{\frac{3}{2}}$–$5f_{\frac{5}{2}}$	1.57E-1	1.571E-1	[7] LS
$3d_{\frac{5}{2}}$–$5f_{\frac{5}{2}}$	7.48E-3	7.480E-3	[7] LS
$3d_{\frac{5}{2}}$–$6p_{\frac{3}{2}}$	1.31E-3	1.29E-3	[4] LS
$3d_{\frac{3}{2}}$–$6p_{\frac{1}{2}}$	1.10E-3	1.08E-3	[4] LS
$3d_{\frac{3}{2}}$–$6p_{\frac{3}{2}}$	2.19E-4	2.15E-4	[4] LS
$3d_{\frac{5}{2}}$–$7p_{\frac{3}{2}}$	6.57E-4	6.46E-4	[4] LS
$3d_{\frac{3}{2}}$–$7p_{\frac{1}{2}}$	5.48E-4	5.39E-4	[4] LS
$3d_{\frac{3}{2}}$–$7p_{\frac{3}{2}}$	1.10E-4	1.08E-4	[4] LS
$3d_{\frac{5}{2}}$–$8p_{\frac{3}{2}}$	3.86E-4	3.75E-4	[4] LS
$3d_{\frac{3}{2}}$–$8p_{\frac{1}{2}}$	3.21E-4	3.13E-4	[4] LS
$3d_{\frac{3}{2}}$–$8p_{\frac{3}{2}}$	6.43E-5	6.25E-5	[4] LS
$4s_{\frac{1}{2}}$–$4p_{\frac{3}{2}}$	1.09	1.095	[3] LS
$4s_{\frac{1}{2}}$–$4p_{\frac{1}{2}}$	5.47E-1	5.477E-1	[3] LS
$4s_{\frac{1}{2}}$–$5p_{\frac{3}{2}}$	6.59E-4	6.35E-4	[4] LS
$4s_{\frac{1}{2}}$–$5p_{\frac{1}{2}}$	3.29E-4	3.17E-4	[4] LS
$4s_{\frac{1}{2}}$–$6p_{\frac{3}{2}}$	1.86E-4	1.94E-4	[4] LS
$4s_{\frac{1}{2}}$–$6p_{\frac{1}{2}}$	9.32E-5	9.70E-5	[4] LS
$4s_{\frac{1}{2}}$–$7p_{\frac{3}{2}}$	3.25E-4	3.24E-4	[4] LS
$4s_{\frac{1}{2}}$–$7p_{\frac{1}{2}}$	1.62E-4	1.62E-4	[4] LS
$4s_{\frac{1}{2}}$–$8p_{\frac{3}{2}}$	3.11E-4	2.91E-4	[4] LS
$4s_{\frac{1}{2}}$–$8p_{\frac{1}{2}}$	1.56E-4	1.45E-4	[4] LS
$4p_{\frac{3}{2}}$–$4d_{\frac{5}{2}}$	1.22E-1	1.209E-1	[3] LS
$4p_{\frac{1}{2}}$–$4d_{\frac{3}{2}}$	1.36E-1	1.343E-1	[3] LS
$4p_{\frac{3}{2}}$–$4d_{\frac{3}{2}}$	1.36E-2	1.343E-2	[3] LS
$4p_{\frac{3}{2}}$–$5s_{\frac{1}{2}}$	3.36E-1	3.35E-1	[4] LS
$4p_{\frac{1}{2}}$–$5s_{\frac{1}{2}}$	3.36E-1	3.35E-1	[4] LS
$4p_{\frac{3}{2}}$–$5d_{\frac{5}{2}}$	4.42E-1	4.45E-1	[4] LS
$4p_{\frac{1}{2}}$–$5d_{\frac{3}{2}}$	4.91E-1	4.95E-1	[4] LS
$4p_{\frac{3}{2}}$–$5d_{\frac{3}{2}}$	4.91E-2	4.95E-2	[4] LS
$4p_{\frac{3}{2}}$–$6s_{\frac{1}{2}}$	3.86E-2	3.87E-2	[4] LS
$4p_{\frac{1}{2}}$–$6s_{\frac{1}{2}}$	3.86E-2	3.87E-2	[4] LS
$4p_{\frac{3}{2}}$–$6d_{\frac{5}{2}}$	1.19E-1	1.20E-1	[4] LS
$4p_{\frac{1}{2}}$–$6d_{\frac{3}{2}}$	1.32E-1	1.33E-1	[4] LS
$4p_{\frac{3}{2}}$–$6d_{\frac{3}{2}}$	1.32E-2	1.33E-2	[4] LS
$4p_{\frac{3}{2}}$–$7s_{\frac{1}{2}}$	1.32E-2	1.33E-2	[4] LS
$4p_{\frac{1}{2}}$–$7s_{\frac{1}{2}}$	1.32E-2	1.33E-2	[4] LS
$4p_{\frac{3}{2}}$–$7d_{\frac{5}{2}}$	5.22E-2	5.24E-2	[4] LS
$4p_{\frac{1}{2}}$–$7d_{\frac{3}{2}}$	5.80E-2	5.83E-2	[4] LS
$4p_{\frac{3}{2}}$–$7d_{\frac{3}{2}}$	5.80E-3	5.83E-3	[4] LS
$4p_{\frac{3}{2}}$–$8s_{\frac{1}{2}}$	6.41E-3	6.42E-3	[4] LS
$4p_{\frac{1}{2}}$–$8s_{\frac{1}{2}}$	6.41E-3	6.42E-3	[4] LS
$4p_{\frac{3}{2}}$–$8d_{\frac{5}{2}}$	2.84E-2	2.84E-2	[4] LS
$4p_{\frac{1}{2}}$–$8d_{\frac{3}{2}}$	3.15E-2	3.15E-2	[4] LS
$4p_{\frac{3}{2}}$–$8d_{\frac{3}{2}}$	3.15E-3	3.15E-3	[4] LS

Table 3. continued.

Transition	This work	Other works	
$4d_{\frac{5}{2}}$–$5p_{\frac{3}{2}}$	4.41E-2	4.35E-2	[4] LS
$4d_{\frac{3}{2}}$–$5p_{\frac{1}{2}}$	3.68E-2	3.62E-2	[4] LS
$4d_{\frac{3}{2}}$–$5p_{\frac{3}{2}}$	7.36E-3	7.25E-3	[4] LS
$4d_{\frac{5}{2}}$–$6p_{\frac{3}{2}}$	8.76E-3	8.65E-3	[4] LS
$4d_{\frac{3}{2}}$–$6p_{\frac{1}{2}}$	7.30E-3	7.21E-3	[4] LS
$4d_{\frac{3}{2}}$–$6p_{\frac{3}{2}}$	1.46E-3	1.44E-3	[4] LS
$4d_{\frac{5}{2}}$–$7p_{\frac{3}{2}}$	3.38E-3	3.33E-3	[4] LS
$4d_{\frac{3}{2}}$–$7p_{\frac{1}{2}}$	2.82E-3	2.78E-3	[4] LS
$4d_{\frac{3}{2}}$–$7p_{\frac{3}{2}}$	5.63E-4	5.55E-4	[4] LS
$4d_{\frac{5}{2}}$–$8p_{\frac{3}{2}}$	1.73E-3	1.68E-3	[4] LS
$4d_{\frac{3}{2}}$–$8p_{\frac{1}{2}}$	1.44E-3	1.40E-3	[4] LS
$4d_{\frac{3}{2}}$–$8p_{\frac{3}{2}}$	2.88E-4	2.80E-4	[4] LS
$5s_{\frac{1}{2}}$–$5p_{\frac{3}{2}}$	1.37	1.37	[4] LS
$5s_{\frac{1}{2}}$–$5p_{\frac{1}{2}}$	6.84E-1	6.85E-1	[4] LS
$5s_{\frac{1}{2}}$–$6p_{\frac{3}{2}}$	2.32E-3	2.28E-3	[4] LS
$5s_{\frac{1}{2}}$–$6p_{\frac{1}{2}}$	1.16E-3	1.14E-3	[4] LS
$5s_{\frac{1}{2}}$–$8p_{\frac{3}{2}}$	1.37E-4	1.16E-4	[4] LS
$5s_{\frac{1}{2}}$–$8p_{\frac{1}{2}}$	6.83E-5	5.82E-5	[4] LS
$5p_{\frac{3}{2}}$–$5d_{\frac{5}{2}}$	1.72E-1	1.71E-1	[4] LS
$5p_{\frac{1}{2}}$–$5d_{\frac{3}{2}}$	1.91E-1	1.90E-1	[4] LS
$5p_{\frac{3}{2}}$–$5d_{\frac{3}{2}}$	1.91E-2	1.90E-2	[4] LS
$5p_{\frac{3}{2}}$–$6s_{\frac{1}{2}}$	4.48E-1	4.49E-1	[4] LS
$5p_{\frac{1}{2}}$–$6s_{\frac{1}{2}}$	4.48E-1	4.49E-1	[4] LS
$5p_{\frac{3}{2}}$–$6d_{\frac{5}{2}}$	4.39E-1	4.44E-1	[4] LS
$5p_{\frac{1}{2}}$–$6d_{\frac{3}{2}}$	4.88E-1	4.93E-1	[4] LS
$5p_{\frac{3}{2}}$–$6d_{\frac{3}{2}}$	4.88E-2	4.93E-2	[4] LS
$5p_{\frac{3}{2}}$–$7s_{\frac{1}{2}}$	5.10E-2	5.11E-2	[4] LS
$5p_{\frac{1}{2}}$–$7s_{\frac{1}{2}}$	5.10E-2	5.11E-2	[4] LS
$5p_{\frac{3}{2}}$–$7d_{\frac{5}{2}}$	1.22E-1	1.23E-1	[4] LS
$5p_{\frac{1}{2}}$–$7d_{\frac{3}{2}}$	1.36E-1	1.37E-1	[4] LS
$5p_{\frac{3}{2}}$–$7d_{\frac{3}{2}}$	1.36E-2	1.37E-2	[4] LS
$5p_{\frac{3}{2}}$–$8s_{\frac{1}{2}}$	1.74E-2	1.75E-2	[4] LS
$5p_{\frac{1}{2}}$–$8s_{\frac{1}{2}}$	1.74E-2	1.75E-2	[4] LS
$5p_{\frac{3}{2}}$–$8d_{\frac{5}{2}}$	5.48E-2	5.50E-2	[4] LS
$5p_{\frac{1}{2}}$–$8d_{\frac{3}{2}}$	6.09E-2	6.11E-2	[4] LS
$5p_{\frac{3}{2}}$–$8d_{\frac{3}{2}}$	6.09E-3	6.11E-3	[4] LS
$5d_{\frac{5}{2}}$–$6p_{\frac{3}{2}}$	7.43E-2	7.32E-2	[4] LS
$5d_{\frac{3}{2}}$–$6p_{\frac{1}{2}}$	6.19E-2	6.10E-2	[4] LS
$5d_{\frac{3}{2}}$–$6p_{\frac{3}{2}}$	1.24E-2	1.22E-2	[4] LS
$5d_{\frac{5}{2}}$–$7p_{\frac{3}{2}}$	1.51E-2	1.49E-2	[4] LS
$5d_{\frac{3}{2}}$–$7p_{\frac{1}{2}}$	1.26E-2	1.24E-2	[4] LS
$5d_{\frac{3}{2}}$–$7p_{\frac{3}{2}}$	2.51E-3	2.48E-3	[4] LS
$5d_{\frac{5}{2}}$–$8p_{\frac{3}{2}}$	5.93E-3	5.79E-3	[4] LS
$5d_{\frac{3}{2}}$–$8p_{\frac{1}{2}}$	4.94E-3	4.82E-3	[4] LS
$5d_{\frac{3}{2}}$–$8p_{\frac{3}{2}}$	9.88E-4	9.65E-4	[4] LS
$6s_{\frac{1}{2}}$–$6p_{\frac{3}{2}}$	1.64	1.64	[4] LS
$6s_{\frac{1}{2}}$–$6p_{\frac{1}{2}}$	8.19E-1	8.19E-1	[4] LS
$6s_{\frac{1}{2}}$–$7p_{\frac{3}{2}}$	4.30E-3	4.31E-3	[4] LS
$6s_{\frac{1}{2}}$–$7p_{\frac{1}{2}}$	2.15E-3	2.15E-3	[4] LS
$6p_{\frac{3}{2}}$–$6d_{\frac{5}{2}}$	2.18E-1	2.20E-1	[4] LS
$6p_{\frac{1}{2}}$–$6d_{\frac{3}{2}}$	2.42E-1	2.44E-1	[4] LS

Table 3. continued.

Transition	This work	Other works	
$6p_{\frac{3}{2}}$–$6d_{\frac{3}{2}}$	2.42E-2	2.44E-2	[4] LS
$6p_{\frac{3}{2}}$–$7s_{\frac{1}{2}}$	5.61E-1	5.61E-1	[4] LS
$6p_{\frac{1}{2}}$–$7s_{\frac{1}{2}}$	5.61E-1	5.61E-1	[4] LS
$6p_{\frac{3}{2}}$–$7d_{\frac{5}{2}}$	4.48E-1	4.54E-1	[4] LS
$6p_{\frac{1}{2}}$–$7d_{\frac{3}{2}}$	4.98E-1	5.05E-1	[4] LS
$6p_{\frac{3}{2}}$–$7d_{\frac{3}{2}}$	4.98E-2	5.05E-2	[4] LS
$6p_{\frac{3}{2}}$–$8s_{\frac{1}{2}}$	6.31E-2	6.32E-2	[4] LS
$6p_{\frac{1}{2}}$–$8s_{\frac{1}{2}}$	6.31E-2	6.32E-2	[4] LS
$6p_{\frac{3}{2}}$–$8d_{\frac{5}{2}}$	1.27E-1	1.27E-1	[4] LS
$6p_{\frac{1}{2}}$–$8d_{\frac{3}{2}}$	1.41E-1	1.41E-1	[4] LS
$6p_{\frac{3}{2}}$–$8d_{\frac{3}{2}}$	1.41E-2	1.41E-2	[4] LS
$6d_{\frac{5}{2}}$–$7p_{\frac{3}{2}}$	1.07E-1	1.05E-1	[4] LS
$6d_{\frac{3}{2}}$–$7p_{\frac{1}{2}}$	8.93E-2	8.74E-2	[4] LS
$6d_{\frac{3}{2}}$–$7p_{\frac{3}{2}}$	1.79E-2	1.75E-2	[4] LS
$6d_{\frac{5}{2}}$–$8p_{\frac{3}{2}}$	2.22E-2	2.17E-2	[4] LS
$6d_{\frac{3}{2}}$–$8p_{\frac{1}{2}}$	1.85E-2	1.81E-2	[4] LS
$6d_{\frac{3}{2}}$–$8p_{\frac{3}{2}}$	3.70E-3	3.61E-3	[4] LS
$7s_{\frac{1}{2}}$–$7p_{\frac{3}{2}}$	1.91	1.91	[4] LS
$7s_{\frac{1}{2}}$–$7p_{\frac{1}{2}}$	9.53E-1	9.55E-1	[4] LS
$7s_{\frac{1}{2}}$–$8p_{\frac{3}{2}}$	6.15E-3	6.54E-3	[4] LS
$7s_{\frac{1}{2}}$–$8p_{\frac{1}{2}}$	3.07E-3	3.27E-3	[4] LS
$7p_{\frac{3}{2}}$–$7d_{\frac{5}{2}}$	2.64E-1	2.64E-1	[4] LS
$7p_{\frac{1}{2}}$–$7d_{\frac{3}{2}}$	2.94E-1	2.93E-1	[4] LS
$7p_{\frac{3}{2}}$–$7d_{\frac{3}{2}}$	2.94E-2	2.93E-2	[4] LS
$7p_{\frac{3}{2}}$–$8s_{\frac{1}{2}}$	6.73E-1	6.74E-1	[4] LS
$7p_{\frac{1}{2}}$–$8s_{\frac{1}{2}}$	6.73E-1	6.74E-1	[4] LS
$7p_{\frac{3}{2}}$–$8d_{\frac{5}{2}}$	4.66E-1	4.69E-1	[4] LS
$7p_{\frac{1}{2}}$–$8d_{\frac{3}{2}}$	5.18E-1	5.21E-1	[4] LS
$7p_{\frac{3}{2}}$–$8d_{\frac{3}{2}}$	5.18E-2	5.21E-2	[4] LS
$7d_{\frac{5}{2}}$–$8p_{\frac{3}{2}}$	1.43E-1	1.39E-1	[4] LS
$7d_{\frac{3}{2}}$–$8p_{\frac{1}{2}}$	1.19E-1	1.16E-1	[4] LS
$7d_{\frac{3}{2}}$–$8p_{\frac{3}{2}}$	2.38E-2	2.31E-2	[4] LS
$8s_{\frac{1}{2}}$–$8p_{\frac{3}{2}}$	2.17	2.17	[4] LS
$8s_{\frac{1}{2}}$–$8p_{\frac{1}{2}}$	1.08	1.09	[4] LS
$8p_{\frac{3}{2}}$–$8d_{\frac{5}{2}}$	3.10E-1	3.10E-1	[4] LS
$8p_{\frac{1}{2}}$–$8d_{\frac{3}{2}}$	3.45E-1	3.44E-1	[4] LS
$8p_{\frac{3}{2}}$–$8d_{\frac{3}{2}}$	3.45E-2	3.44E-2	[4] LS

References. [1]: High precision calculations using variational wave functions in Hylleraas coordinates, Yan & Drake (1995); [2]: multi-configuration Hantree-Fock calculations, Fischer et al. (1998); [3]: results of the superposition of correlated configurations method, Pestka & Woznicki (1996); [4]: close-coupling calculations, Peach et al. (1988); [5]: Filippov (1931); [6]: full-core-plus-correlation method, Qu et al. (1997); [7]: full-core-plus-correlation method, Qu et al. (1999). LS: The transition probability for this line was calculated from the multiplet value assuming a pure LS-coupling.

Table 4. QDT-calculated oscillator strengths f_{ik} and transition probabilities A_{ki} for the transition involving nd, nf, ng, and nh states of Li I.

Transition i–k	Lower level (cm^{-1})	Upper level (cm^{-1})	ν (cm^{-1})	λ (nm)	f_{ik}	log($g_i f_{ik}$)	A_{ki} (s^{-1})
$7h_{\frac{9}{2}}$–$8g_{\frac{9}{2}}$	41 247.812	41 771.9 [2]	524.088	19 075.6	3.87×10^{-4}	−5.55	7.10×10^{1}
$7h_{\frac{9}{2}}$–$8g_{\frac{7}{2}}$	41 247.812	41 771.9 [2]	524.088	19 075.6	1.70×10^{-2}	−1.77	3.90×10^{3}
$7h_{\frac{11}{2}}$–$8g_{\frac{9}{2}}$	41 247.812	41 771.9 [2]	524.088	19 075.6	1.74×10^{-2}	−1.57	3.83×10^{3}
$7g_{\frac{9}{2}}$–$8h_{\frac{9}{2}}$	41 246.8 [2]	41 771.91 [2]	525.11	19 038.4	2.65×10^{-2}	−1.33	4.88×10^{3}
$7g_{\frac{9}{2}}$–$8h_{\frac{11}{2}}$	41 246.8 [2]	41 771.91 [2]	525.11	19 038.4	1.43	+2.66	2.20×10^{5}
$7g_{\frac{7}{2}}$–$8h_{\frac{9}{2}}$	41 246.8 [2]	41 771.91 [2]	525.11	19 038.4	1.46	+2.46	2.15×10^{5}
$6f_{\frac{7}{2}}$–$7d_{\frac{5}{2}}$	40 438.9 [1]	41 246.5 [3]	807.6	12 379.0	4.22×10^{-2}	−1.09	2.45×10^{4}
$6f_{\frac{5}{2}}$–$7d_{\frac{5}{2}}$	40 438.9 [1]	41 246.5 [3]	807.6	12 379.0	2.81×10^{-3}	−4.08	1.22×10^{3}
$6f_{\frac{5}{2}}$–$7d_{\frac{3}{2}}$	40 438.9 [1]	41 246.5 [3]	807.6	12 379.0	3.94×10^{-2}	−1.44	2.57×10^{4}
$6h_{\frac{9}{2}}$–$7g_{\frac{9}{2}}$	40 439.152	41 246.8 [2]	807.648	12 378.3	1.40×10^{-4}	−6.57	6.07×10^{1}
$6h_{\frac{9}{2}}$–$7g_{\frac{7}{2}}$	40 439.152	41 246.8 [2]	807.648	12 378.3	6.14×10^{-3}	−2.79	3.34×10^{3}
$6h_{\frac{11}{2}}$–$7g_{\frac{9}{2}}$	40 439.152	41 246.8 [2]	807.648	12 378.3	6.28×10^{-3}	−2.59	3.28×10^{3}
$6f_{\frac{7}{2}}$–$7g_{\frac{9}{2}}$	40 438.9 [1]	41 246.8 [2]	807.9	12 374.4	1.08	+2.16	3.77×10^{5}
$6f_{\frac{7}{2}}$–$7g_{\frac{7}{2}}$	40 438.9 [1]	41 246.8 [2]	807.9	12 374.4	3.10×10^{-2}	−1.39	1.35×10^{4}
$6f_{\frac{5}{2}}$–$7g_{\frac{7}{2}}$	40 438.9 [1]	41 246.8 [2]	807.9	12 374.4	1.11	+1.9	3.64×10^{5}
$6g_{\frac{9}{2}}$–$7h_{\frac{9}{2}}$	40 438.892	41 247.812	808.92	12 358.8	2.71×10^{-2}	−1.31	1.18×10^{4}
$6g_{\frac{9}{2}}$–$7h_{\frac{11}{2}}$	40 438.892	41 247.812	808.92	12 358.8	1.46	+2.68	5.32×10^{5}
$6g_{\frac{7}{2}}$–$7h_{\frac{9}{2}}$	40 438.892	41 247.812	808.92	12 358.8	1.49	+2.48	5.20×10^{5}
$6f_{\frac{7}{2}}$–$8d_{\frac{5}{2}}$	40 438.9 [1]	41 771.3 [3]	1332.4	7503.21	8.46×10^{-3}	−2.69	1.34×10^{4}
$6f_{\frac{5}{2}}$–$8d_{\frac{5}{2}}$	40 438.9 [1]	41 771.3 [3]	1332.4	7503.21	5.64×10^{-4}	−5.69	6.68×10^{2}
$6f_{\frac{5}{2}}$–$8d_{\frac{3}{2}}$	40 438.9 [1]	41 771.3 [3]	1332.4	7503.21	7.89×10^{-3}	−3.05	1.40×10^{4}
$6h_{\frac{9}{2}}$–$8g_{\frac{9}{2}}$	40 439.152	41 771.9 [2]	1332.748	7501.25	1.91×10^{-5}	−8.56	2.26×10^{1}
$6h_{\frac{9}{2}}$–$8g_{\frac{7}{2}}$	40 439.152	41 771.9 [2]	1332.748	7501.25	8.40×10^{-4}	−4.78	1.24×10^{3}
$6h_{\frac{11}{2}}$–$8g_{\frac{9}{2}}$	40 439.152	41 771.9 [2]	1332.748	7501.25	8.59×10^{-4}	−4.57	1.22×10^{3}
$6f_{\frac{7}{2}}$–$8g_{\frac{9}{2}}$	40 438.9 [1]	41 771.9 [2]	1333.	7499.83	2.39×10^{-1}	+0.648	2.26×10^{5}
$6f_{\frac{7}{2}}$–$8g_{\frac{7}{2}}$	40 438.9 [1]	41 771.9 [2]	1333.	7499.83	6.82×10^{-3}	−2.91	8.08×10^{3}
$6f_{\frac{5}{2}}$–$8g_{\frac{7}{2}}$	40 438.9 [1]	41 771.9 [2]	1333.	7499.83	2.46×10^{-1}	+0.389	2.18×10^{5}
$6g_{\frac{9}{2}}$–$8h_{\frac{9}{2}}$	40 438.892	41 771.91 [2]	1333.018	7499.73	5.02×10^{-3}	−2.99	5.95×10^{3}
$6g_{\frac{9}{2}}$–$8h_{\frac{11}{2}}$	40 438.892	41 771.91 [2]	1333.018	7499.73	2.71×10^{-1}	+0.997	2.68×10^{5}
$6g_{\frac{7}{2}}$–$8h_{\frac{9}{2}}$	40 438.892	41 771.91 [2]	1333.018	7499.73	2.76×10^{-1}	+0.792	2.62×10^{5}
$5f_{\frac{7}{2}}$–$6d_{\frac{5}{2}}$	39 097.503 [1]	40 437.22 [1]	1339.717	7462.23	2.37×10^{-2}	−1.66	3.79×10^{4}
$5f_{\frac{5}{2}}$–$6d_{\frac{5}{2}}$	39 097.499 [1]	40 437.22 [1]	1339.721	7462.21	1.58×10^{-3}	−4.66	1.89×10^{3}
$5f_{\frac{5}{2}}$–$6d_{\frac{3}{2}}$	39 097.499 [1]	40 437.22 [1]	1339.721	7462.21	2.22×10^{-2}	−2.02	3.98×10^{4}
$5g_{\frac{9}{2}}$–$6f_{\frac{7}{2}}$	39 097.941 [1]	40 438.9 [1]	1340.959	7455.32	7.40×10^{-3}	−2.6	1.11×10^{4}
$5g_{\frac{7}{2}}$–$6f_{\frac{7}{2}}$	39 097.941 [1]	40 438.9 [1]	1340.959	7455.32	2.64×10^{-4}	−6.16	3.17×10^{2}
$5g_{\frac{7}{2}}$–$6f_{\frac{5}{2}}$	39 097.941 [1]	40 438.9 [1]	1340.959	7455.32	7.13×10^{-3}	−2.86	1.14×10^{4}
$5g_{\frac{9}{2}}$–$6h_{\frac{9}{2}}$	39 097.941 [1]	40 439.152	*1341.211*	7453.92	3.05×10^{-2}	−1.19	3.66×10^{4}
$5g_{\frac{9}{2}}$–$6h_{\frac{11}{2}}$	39 097.941 [1]	40 439.152	*1341.211*	7453.92	1.65	+2.8	1.65×10^{6}
$5g_{\frac{7}{2}}$–$6h_{\frac{9}{2}}$	39 097.941 [1]	40 439.152	*1341.211*	7453.92	1.68	+2.6	1.61×10^{6}
$5f_{\frac{7}{2}}$–$6g_{\frac{9}{2}}$	39 097.503 [1]	40 438.997	*1341.494*	7454.38	1.15	+2.22	1.11×10^{6}
$5f_{\frac{7}{2}}$–$6g_{\frac{7}{2}}$	39 097.503 [1]	40 438.997	*1341.494*	7454.38	3.29×10^{-2}	−1.33	3.95×10^{4}
$5f_{\frac{5}{2}}$–$6g_{\frac{7}{2}}$	39 097.499 [1]	40 438.997	*1341.494*	7454.38	1.19	+1.97	1.07×10^{6}
$5d_{\frac{5}{2}}$–$6f_{\frac{7}{2}}$	39 094.869 [1]	40 438.9 [1]	1344.031	7438.28	7.99×10^{-1}	+1.57	7.22×10^{5}
$5d_{\frac{5}{2}}$–$6f_{\frac{5}{2}}$	39 094.869 [1]	40 438.9 [1]	1344.031	7438.28	4.00×10^{-2}	−1.43	4.82×10^{4}
$5d_{\frac{3}{2}}$–$6f_{\frac{5}{2}}$	39 094.861 [1]	40 438.9 [1]	1344.039	7438.23	8.39×10^{-1}	+1.21	6.74×10^{5}
$6f_{\frac{7}{2}}$–$9d_{\frac{5}{2}}$	40 438.9 [1]	42 131.3 [3]	1692.4	5907.16	3.20×10^{-3}	−3.67	8.15×10^{3}
$6f_{\frac{5}{2}}$–$9d_{\frac{5}{2}}$	40 438.9 [1]	42 131.3 [3]	1692.4	5907.16	2.13×10^{-4}	−6.66	4.07×10^{2}
$6f_{\frac{5}{2}}$–$9d_{\frac{3}{2}}$	40 438.9 [1]	42 131.3 [3]	1692.4	5907.16	2.99×10^{-3}	−4.02	8.56×10^{3}

Notes. The energy levels are taken from Table 1 except for cited values. The italicized wavenumbers correspond to the lines experimentally observed in the present work (see Table 1). The air wavelengths are specified.

Table 4. continued.

Transition i–k	Lower level (cm^{-1})	Upper level (cm^{-1})	ν (cm^{-1})	λ (nm)	f_{ik}	$\log(g_i f_{ik})$	A_{ki} (s^{-1})
$6f_{\frac{7}{2}}$–$10d_{\frac{5}{2}}$	40 438.9 [1]	42 389. [3]	1950.1	5126.54	1.59×10^{-3}	−4.36	5.37×10^{3}
$6f_{\frac{5}{2}}$–$10d_{\frac{5}{2}}$	40 438.9 [1]	42 389. [3]	1950.1	5126.54	1.06×10^{-4}	−7.36	2.69×10^{2}
$6f_{\frac{5}{2}}$–$10d_{\frac{3}{2}}$	40 438.9 [1]	42 389. [3]	1950.1	5126.54	1.48×10^{-3}	−4.72	5.64×10^{3}
$6f_{\frac{7}{2}}$–$11d_{\frac{5}{2}}$	40 438.9 [1]	42 578. [3]	2139.1	4673.59	1.02×10^{-3}	−4.81	4.13×10^{3}
$6f_{\frac{5}{2}}$–$11d_{\frac{5}{2}}$	40 438.9 [1]	42 578. [3]	2139.1	4673.59	6.77×10^{-5}	−7.81	2.07×10^{2}
$6f_{\frac{5}{2}}$–$11d_{\frac{3}{2}}$	40 438.9 [1]	42 578. [3]	2139.1	4673.59	9.48×10^{-4}	−5.17	4.34×10^{3}
$5f_{\frac{7}{2}}$–$7d_{\frac{5}{2}}$	39 097.503 [1]	41 246.5 [3]	2148.997	4652.07	4.52×10^{-3}	−3.32	1.86×10^{4}
$5f_{\frac{5}{2}}$–$7d_{\frac{5}{2}}$	39 097.499 [1]	41 246.5 [3]	2149.001	4652.06	3.01×10^{-4}	−6.32	9.28×10^{2}
$5f_{\frac{5}{2}}$–$7d_{\frac{3}{2}}$	39 097.499 [1]	41 246.5 [3]	2149.001	4652.06	4.22×10^{-3}	−3.68	1.95×10^{4}
$5f_{\frac{7}{2}}$–$7g_{\frac{9}{2}}$	39 097.503 [1]	41 246.8 [2]	2149.297	4651.42	2.22×10^{-1}	+0.574	5.48×10^{5}
$5f_{\frac{7}{2}}$–$7g_{\frac{7}{2}}$	39 097.503 [1]	41 246.8 [2]	2149.297	4651.42	6.35×10^{-3}	−2.98	1.96×10^{4}
$5f_{\frac{5}{2}}$–$7g_{\frac{7}{2}}$	39 097.499 [1]	41 246.8 [2]	2149.301	4651.41	2.29×10^{-1}	+0.318	5.28×10^{5}
$5g_{\frac{9}{2}}$–$7h_{\frac{9}{2}}$	39 097.941 [1]	41 247.812	*2149.871*	4650.17	3.67×10^{-3}	−3.3	1.13×10^{4}
$5g_{\frac{9}{2}}$–$7h_{\frac{11}{2}}$	39 097.941 [1]	41 247.812	*2149.871*	4650.17	1.98×10^{-1}	+0.683	5.09×10^{5}
$5g_{\frac{7}{2}}$–$7h_{\frac{9}{2}}$	39 097.941 [1]	41 247.812	*2149.871*	4650.17	2.02×10^{-1}	+0.48	4.97×10^{5}
$6f_{\frac{7}{2}}$–$12d_{\frac{5}{2}}$	40 438.9 [1]	42 725. [3]	2286.1	4373.07	5.73×10^{-4}	−5.39	2.66×10^{3}
$6f_{\frac{5}{2}}$–$12d_{\frac{5}{2}}$	40 438.9 [1]	42 725. [3]	2286.1	4373.07	3.82×10^{-5}	−8.38	1.33×10^{2}
$6f_{\frac{5}{2}}$–$12d_{\frac{3}{2}}$	40 438.9 [1]	42 725. [3]	2286.1	4373.07	5.35×10^{-4}	−5.74	2.80×10^{3}
$4f_{\frac{5}{2}}$–$5d_{\frac{3}{2}}$	36 628.329 [1]	39 094.861 [1]	2466.532	4053.17	8.46×10^{-3}	−2.98	5.15×10^{4}
$4f_{\frac{7}{2}}$–$5d_{\frac{5}{2}}$	36 628.336 [1]	39 094.869 [1]	2466.533	4053.17	9.06×10^{-3}	−2.62	4.90×10^{4}
$4f_{\frac{5}{2}}$–$5d_{\frac{5}{2}}$	36 628.329 [1]	39 094.869 [1]	2466.54	4053.16	6.04×10^{-4}	−5.62	2.45×10^{3}
$4f_{\frac{7}{2}}$–$5g_{\frac{9}{2}}$	36 628.336 [1]	39 097.941 [1]	2469.605	4048.13	1.31	+2.35	4.26×10^{6}
$4f_{\frac{7}{2}}$–$5g_{\frac{7}{2}}$	36 628.336 [1]	39 097.941 [1]	2469.605	4048.13	3.74×10^{-2}	−1.21	1.52×10^{5}
$4f_{\frac{5}{2}}$–$5g_{\frac{7}{2}}$	36 628.329 [1]	39 097.941 [1]	2469.612	4048.12	1.35	+2.09	4.11×10^{6}
$4d_{\frac{5}{2}}$–$5f_{\frac{5}{2}}$	36 623.351 [1]	39 097.499 [1]	2474.148	4040.69	4.22×10^{-2}	−1.37	1.72×10^{5}
$4d_{\frac{5}{2}}$–$5f_{\frac{7}{2}}$	36 623.351 [1]	39 097.503 [1]	2474.152	4040.69	8.44×10^{-1}	+1.62	2.59×10^{6}
$4d_{\frac{3}{2}}$–$5f_{\frac{5}{2}}$	36 623.336 [1]	39 097.499 [1]	2474.163	4040.67	8.87×10^{-1}	+1.27	2.41×10^{6}
$5f_{\frac{7}{2}}$–$8d_{\frac{5}{2}}$	39 097.503 [1]	41 771.3 [3]	2673.797	3738.98	1.68×10^{-3}	−4.31	1.07×10^{4}
$5f_{\frac{5}{2}}$–$8d_{\frac{5}{2}}$	39 097.499 [1]	41 771.3 [3]	2673.801	3738.97	1.12×10^{-4}	−7.31	5.35×10^{2}
$5f_{\frac{5}{2}}$–$8d_{\frac{3}{2}}$	39 097.499 [1]	41 771.3 [3]	2673.801	3738.97	1.57×10^{-3}	−4.66	1.12×10^{4}
$5g_{\frac{9}{2}}$–$8h_{\frac{9}{2}}$	39 097.941 [1]	41 771.91 [2]	2673.969	3738.74	1.12×10^{-3}	−4.49	5.34×10^{3}
$5g_{\frac{9}{2}}$–$8h_{\frac{11}{2}}$	39 097.941 [1]	41 771.91 [2]	2673.969	3738.74	6.04×10^{-2}	−0.504	2.40×10^{5}
$5g_{\frac{7}{2}}$–$8h_{\frac{9}{2}}$	39 097.941 [1]	41 771.91 [2]	2673.969	3738.74	6.15×10^{-2}	−0.709	2.35×10^{5}
$5f_{\frac{7}{2}}$–$8g_{\frac{9}{2}}$	39 097.503 [1]	41 771.9 [2]	2674.397	3738.14	8.20×10^{-2}	−0.422	3.13×10^{5}
$5f_{\frac{7}{2}}$–$8g_{\frac{7}{2}}$	39 097.503 [1]	41 771.9 [2]	2674.397	3738.14	2.34×10^{-3}	−3.98	1.12×10^{4}
$5f_{\frac{5}{2}}$–$8g_{\frac{7}{2}}$	39 097.499 [1]	41 771.9 [2]	2674.401	3738.14	8.43×10^{-2}	−0.682	3.02×10^{5}
$5f_{\frac{7}{2}}$–$9d_{\frac{5}{2}}$	39 097.503 [1]	42 131.3 [3]	3033.797	3295.30	8.32×10^{-4}	−5.01	6.81×10^{3}
$5f_{\frac{5}{2}}$–$9d_{\frac{5}{2}}$	39 097.499 [1]	42 131.3 [3]	3033.801	3295.30	5.54×10^{-5}	−8.01	3.40×10^{2}
$5f_{\frac{5}{2}}$–$9d_{\frac{3}{2}}$	39 097.499 [1]	42 131.3 [3]	3033.801	3295.30	7.76×10^{-4}	−5.37	7.15×10^{3}
$5f_{\frac{7}{2}}$–$10d_{\frac{5}{2}}$	39 097.503 [1]	42 389. [3]	3291.497	3037.30	4.78×10^{-4}	−5.57	4.61×10^{3}
$5f_{\frac{5}{2}}$–$10d_{\frac{5}{2}}$	39 097.499 [1]	42 389. [3]	3291.501	3037.30	3.19×10^{-5}	−8.56	2.30×10^{2}
$5f_{\frac{5}{2}}$–$10d_{\frac{3}{2}}$	39 097.499 [1]	42 389. [3]	3291.501	3037.30	4.46×10^{-4}	−5.92	4.84×10^{3}
$5f_{\frac{7}{2}}$–$11d_{\frac{5}{2}}$	39 097.503 [1]	42 578. [3]	3480.497	2872.37	3.39×10^{-4}	−5.91	3.65×10^{3}
$5f_{\frac{5}{2}}$–$11d_{\frac{5}{2}}$	39 097.499 [1]	42 578. [3]	3480.501	2872.37	2.26×10^{-5}	−8.91	1.82×10^{2}
$5f_{\frac{5}{2}}$–$11d_{\frac{3}{2}}$	39 097.499 [1]	42 578. [3]	3480.501	2872.37	3.16×10^{-4}	−6.27	3.83×10^{3}
$5f_{\frac{7}{2}}$–$12d_{\frac{5}{2}}$	39 097.503 [1]	42 725. [3]	3627.497	2755.97	2.01×10^{-4}	−6.43	2.35×10^{3}
$5f_{\frac{5}{2}}$–$12d_{\frac{5}{2}}$	39 097.499 [1]	42 725. [3]	3627.501	2755.97	1.34×10^{-5}	−9.43	1.18×10^{2}
$5f_{\frac{5}{2}}$–$12d_{\frac{3}{2}}$	39 097.499 [1]	42 725. [3]	3627.501	2755.97	1.88×10^{-4}	−6.79	2.47×10^{3}
$4f_{\frac{7}{2}}$–$6d_{\frac{5}{2}}$	36 628.336 [1]	40 437.22 [1]	3808.884	2624.72	1.62×10^{-3}	−4.35	2.09×10^{4}
$4f_{\frac{5}{2}}$–$6d_{\frac{5}{2}}$	36 628.329 [1]	40 437.22 [1]	3808.891	2624.72	1.08×10^{-4}	−7.34	1.04×10^{3}
$4f_{\frac{5}{2}}$–$6d_{\frac{3}{2}}$	36 628.329 [1]	40 437.22 [1]	3808.891	2624.72	1.51×10^{-3}	−4.7	2.19×10^{4}

Table 4. continued.

Transition i–k	Lower level (cm^{-1})	Upper level (cm^{-1})	ν (cm^{-1})	λ (nm)	f_{ik}	$\log(g_i f_{ik})$	A_{ki} (s^{-1})
$4f_{\frac{7}{2}}$–$6g_{\frac{9}{2}}$	36 628.336 [1]	40 438.892	3810.556	2623.57	1.77×10^{-1}	+0.348	1.37×10^{6}
$4f_{\frac{7}{2}}$–$6g_{\frac{7}{2}}$	36 628.336 [1]	40 438.892	3810.556	2623.57	5.07×10^{-3}	−3.2	4.91×10^{4}
$4f_{\frac{5}{2}}$–$6g_{\frac{7}{2}}$	36 628.329 [1]	40 438.892	3810.563	2623.57	1.82×10^{-1}	+0.088	1.32×10^{6}
$4d_{\frac{5}{2}}$–$6f_{\frac{7}{2}}$	36 623.351 [1]	40 438.9 [1]	3815.549	2620.14	1.77×10^{-1}	+0.0602	1.29×10^{6}
$4d_{\frac{5}{2}}$–$6f_{\frac{5}{2}}$	36 623.351 [1]	40 438.9 [1]	3815.549	2620.14	8.86×10^{-3}	−2.93	8.61×10^{4}
$4d_{\frac{3}{2}}$–$6f_{\frac{5}{2}}$	36 623.336 [1]	40 438.9 [1]	3815.564	2620.13	1.86×10^{-1}	−0.296	1.20×10^{6}
$4f_{\frac{7}{2}}$–$7d_{\frac{5}{2}}$	36 628.336 [1]	41 246.5 [3]	4618.164	2164.77	5.78×10^{-4}	−5.38	1.10×10^{4}
$4f_{\frac{5}{2}}$–$7d_{\frac{5}{2}}$	36 628.329 [1]	41 246.5 [3]	4618.171	2164.77	3.85×10^{-5}	−8.37	5.48×10^{2}
$4f_{\frac{5}{2}}$–$7d_{\frac{3}{2}}$	36 628.329 [1]	41 246.5 [3]	4618.171	2164.77	5.39×10^{-4}	−5.73	1.15×10^{4}
$4f_{\frac{7}{2}}$–$7g_{\frac{9}{2}}$	36 628.336 [1]	41 246.8 [2]	4618.464	2164.63	5.66×10^{-2}	−0.792	6.44×10^{5}
$4f_{\frac{7}{2}}$–$7g_{\frac{7}{2}}$	36 628.336 [1]	41 246.8 [2]	4618.464	2164.63	1.62×10^{-3}	−4.35	2.30×10^{4}
$4f_{\frac{5}{2}}$–$7g_{\frac{7}{2}}$	36 628.329 [1]	41 246.8 [2]	4618.471	2164.63	5.82×10^{-2}	−1.05	6.21×10^{5}
$4f_{\frac{7}{2}}$–$8d_{\frac{5}{2}}$	36 628.336 [1]	41 771.3 [3]	5142.964	1943.87	2.82×10^{-4}	−6.09	6.64×10^{3}
$4f_{\frac{5}{2}}$–$8d_{\frac{5}{2}}$	36 628.329 [1]	41 771.3 [3]	5142.971	1943.87	1.88×10^{-5}	−9.09	3.32×10^{2}
$4f_{\frac{5}{2}}$–$8d_{\frac{3}{2}}$	36 628.329 [1]	41 771.3 [3]	5142.971	1943.87	2.63×10^{-4}	−6.45	6.97×10^{3}
$4f_{\frac{7}{2}}$–$8g_{\frac{9}{2}}$	36 628.336 [1]	41 771.9 [2]	5143.564	1943.65	2.57×10^{-2}	−1.58	3.63×10^{5}
$4f_{\frac{7}{2}}$–$8g_{\frac{7}{2}}$	36 628.336 [1]	41 771.9 [2]	5143.564	1943.65	7.34×10^{-4}	−5.14	1.30×10^{4}
$4f_{\frac{5}{2}}$–$8g_{\frac{7}{2}}$	36 628.329 [1]	41 771.9 [2]	5143.571	1943.64	2.64×10^{-2}	−1.84	3.50×10^{5}
$3d_{\frac{5}{2}}$–$4f_{\frac{5}{2}}$	31 283.087 [1]	36 628.329 [1]	5345.242	1870.31	4.84×10^{-2}	−1.24	9.22×10^{5}
$3d_{\frac{5}{2}}$–$4f_{\frac{7}{2}}$	31 283.087 [1]	36 628.336 [1]	5345.249	1870.31	9.68×10^{-1}	+1.76	1.38×10^{7}
$3d_{\frac{3}{2}}$–$4f_{\frac{5}{2}}$	31 283.051 [1]	36 628.329 [1]	5345.278	1870.30	1.02	+1.41	1.29×10^{7}
$4f_{\frac{7}{2}}$–$9d_{\frac{5}{2}}$	36 628.336 [1]	42 131.3 [3]	5502.964	1816.71	1.62×10^{-4}	−6.65	4.36×10^{3}
$4f_{\frac{5}{2}}$–$9d_{\frac{5}{2}}$	36 628.329 [1]	42 131.3 [3]	5502.971	1816.70	1.08×10^{-5}	−9.64	2.18×10^{2}
$4f_{\frac{5}{2}}$–$9d_{\frac{3}{2}}$	36 628.329 [1]	42 131.3 [3]	5502.971	1816.70	1.51×10^{-4}	−7.01	4.58×10^{3}
$4f_{\frac{7}{2}}$–$10d_{\frac{5}{2}}$	36 628.336 [1]	42 389. [3]	5760.664	1735.44	1.02×10^{-4}	−7.11	3.01×10^{3}
$4f_{\frac{5}{2}}$–$10d_{\frac{5}{2}}$	36 628.329 [1]	42 389. [3]	5760.671	1735.43	6.80×10^{-6}	−10.1	1.51×10^{2}
$4f_{\frac{5}{2}}$–$10d_{\frac{3}{2}}$	36 628.329 [1]	42 389. [3]	5760.671	1735.43	9.52×10^{-5}	−7.47	3.16×10^{3}
$4f_{\frac{7}{2}}$–$11d_{\frac{5}{2}}$	36 628.336 [1]	42 578. [3]	5949.664	1680.31	7.80×10^{-5}	−7.38	2.46×10^{3}
$4f_{\frac{5}{2}}$–$11d_{\frac{5}{2}}$	36 628.329 [1]	42 578. [3]	5949.671	1680.31	5.20×10^{-6}	−10.4	1.23×10^{2}
$4f_{\frac{5}{2}}$–$11d_{\frac{3}{2}}$	36 628.329 [1]	42 578. [3]	5949.671	1680.31	7.28×10^{-5}	−7.74	2.58×10^{3}
$4f_{\frac{7}{2}}$–$12d_{\frac{5}{2}}$	36 628.336 [1]	42 725. [3]	6096.664	1639.79	4.75×10^{-5}	−7.88	1.57×10^{3}
$4f_{\frac{5}{2}}$–$12d_{\frac{5}{2}}$	36 628.329 [1]	42 725. [3]	6096.671	1639.79	3.16×10^{-6}	−10.9	7.84×10^{1}
$4f_{\frac{5}{2}}$–$12d_{\frac{3}{2}}$	36 628.329 [1]	42 725. [3]	6096.671	1639.79	4.43×10^{-5}	−8.23	1.65×10^{3}
$3d_{\frac{5}{2}}$–$5f_{\frac{5}{2}}$	31 283.087 [1]	39 097.499 [1]	7814.412	1279.34	7.48×10^{-3}	−3.1	3.05×10^{5}
$3d_{\frac{5}{2}}$–$5f_{\frac{7}{2}}$	31 283.087 [1]	39 097.503 [1]	7814.416	1279.34	1.50×10^{-1}	−0.105	4.57×10^{6}
$3d_{\frac{3}{2}}$–$5f_{\frac{5}{2}}$	31 283.051 [1]	39 097.499 [1]	7814.449	1279.33	1.57×10^{-1}	−0.465	4.26×10^{6}
$3d_{\frac{5}{2}}$–$6f_{\frac{7}{2}}$	31 283.087 [1]	40 438.9 [1]	9155.813	1091.90	5.15×10^{-2}	−1.17	2.16×10^{6}
$3d_{\frac{5}{2}}$–$6f_{\frac{5}{2}}$	31 283.087 [1]	40 438.9 [1]	9155.813	1091.90	2.58×10^{-3}	−4.17	1.44×10^{5}
$3d_{\frac{3}{2}}$–$6f_{\frac{5}{2}}$	31 283.051 [1]	40 438.9 [1]	9155.85	1091.90	5.41×10^{-2}	−1.53	2.02×10^{6}

References. [1]: Radziemski et al. (1995); [2]: Chen & Wang (2005); [3]: Ralchenko et al. (2011).